Modelling Defects Acceptors And Determination Of Electric Model From The Nyquist Plot And Bode In Thin Film CIGS

Demba Diallo, Moustapha Dieng, Dr. Alain Kassine Ehemba

Abstract: The performance of the chalcopyrite material Cu(In,Ga)Se2 (CIGS) used as an absorber layer in thin-film photovoltaic devices is significantly affected by the presence of native defects. Multivalent defects, e.g. double acceptors or simple acceptor, are important immaterial used in solar cell production in general and in chalcopyrite materials in particular. We used the thin film solar cell simulation software SCAPS to enable the simulation of multivalent defects with up to five different charge states.Algorithms enabled us to simulate an arbitrary number of possible states of load. The presented solution method avoids numerical inaccuracies caused by the subtraction of two almost equal numbers. This new modelling facility is afterwards used to investigate the consequences of the multivalent character of defects for the simulation of chalcopyrite based CIGS. The capacitance increase with the evolution of the number of defects, *C- f* curves have found to have defect dependence.

Index Terms: Defects and acceptors in semiconductor CIGS, numerical modelling, Nyquist plot, SCAPS, Solar cells.

1 Introduction

Multivalent defects, i.e. defects with more than two possible charge states are important in several material systems used in solar cell production [1, 2]. In particular for chalcopyrite materials CIGS, theoretical studies which are in good agreement with measurement results identify most of the existing defects as multivalent defects, e.g. triple defect acceptor, double defect acceptors and simple defect acceptors [3, 4]. The statistics governing this kind of defects differs from the usual Shockley-Read-Hall (SRH) statistics, for defects with only two possible charge states [1]. The object of this article is used the numerical tool for simulation SCAPS for the modelling of the general-purpose defects and the states acceptors in their more general form in the film CIGS. The Nyquist plot and Bode is used for giving some electric parameters. From these parameters, we proposed a model electric equivalent.

2 Definitions and Assumptions

The recombination through defects is often described by the Shockley-Read-Hall (SRH) [5, 6] statistics. The net recombination rate *U*, is considered to be the result of capture and emission processes of holes and electrons (see figure.1). Partially following the notation of Sah and Shockley [1], the different charge states are designated with a subscript s representing the number of electrons on the defect. The most positive charge state corresponds then to s=0, and the most negative to s=H. The different transitions (defect levels) are designated with a superscript which is the mean value of the charge states involved.

- *Demba DIALLO is currently pursuing doctoral degree program in physical sciences in Cheikh Anta Diop University, Dakar/Senegal.*
  E-mail: ddemba00@gmail.com
- *Moustapha DIENG is currently working as an associate professor in department of physics in Cheikh Anta Diop University, Dakar/Senegal.*
- *Dr. Alain Kassine EHEMBA is in department of physics in Cheikh Anta Diop University, Dakar/Senegal.*

For example the density of a defect in state s is noted as Ns, and the recombination rate associated with transitions between the states s and s+1 is noted as $U^{s+1/2}$. The different charge states are indicated at the bottom and the transitions at the top of the figure 2.The most positively charged state corresponds with *s* = 0 in this example.

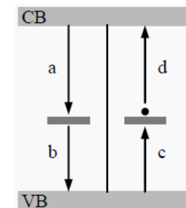

Fig.1. *the basic processes involved in SRH-recombination through an acceptor defect: (a) electron capture; (b) hole emission; (c) hole capture; (d) electron emission. If the defect is in the unoccupied state (left side), processes (a) or (b) can occur leading to an occupied state (right side) and vice versa.*

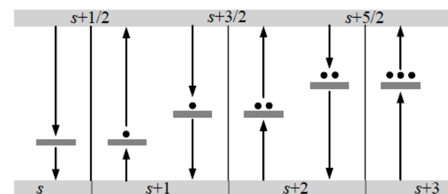

Fig.2. *the basic processes involved in recombination through a multivalent defect with four different charge states (N = 4).*

The arrows represent capture and emission processes in a similar way as in figure 1. The net electron and hole capture rates are noted as $U_n^{s+1/2}$ and $U_p^{s+1/2}$ to (1).

$$\begin{cases} U_n^{s+1/2} = nc_n^{s+1/2} N_s - e_n^{s+1/2} N_{s+1} \\ U_p^{s+1/2} = pc_p^{s+1/2} N_{s+1} - e_p^{s+1/2} N_s \end{cases} \tag{1}$$

IJSTR©2015
www.ijstr.org

3 NUMERICAL PROCEDURES AND ALGORITHMS

In order to calculate the occupation probabilities of the different defect levels continuity has to be to (2).

$$\frac{\partial N_s}{\partial t} = U_n^{s-1/2} - U_n^{s+1/2} - U_p^{s-1/2} + U_p^{s+1/2} \quad (2)$$

This expression doesn't hold for the most negative and positive charged states, e.g. for s=0 and s=1, it should be replaced respectively with equation (3 to 4).

$$\frac{\partial N_0}{\partial t} = -U_n^{1/2} + U_p^{1/2} \quad (3)$$

$$\frac{\partial N_1}{\partial t} = U_n^{1/2} - U_n^{3/2} - U_p^{1/2} + U_p^{3/2} \quad (4)$$

This leads to a system of *N* - 1 independent linear differential equations for *N* unknown functions *Ns*. This system can be completed by demanding that the sum of all charge state densities must equal the total defect density.

$$\sum_{s=0}^{N-1} N_s = N_t \quad (5)$$

4 RESULTS AND DISCUSSIONS

To illustrate the importance of correct multivalent modelling, we start from the 'NUMOS CIGS baseline.def' model [4], which is distributed together with the installation package of SCAPS, and which is a good representative for a CIGS thin film solar cell structure. This structure consists of a 3 µm wide CIGS absorber layer, together with a 50 nm CdS buffer layer and a ZnO window layer. To illustrate the importance of correct multivalent modelling, we start from the 'NUMOS CIGS baseline.def' model [4], which is distributed together with the installation package of SCAPS, and which is a good representative for a CIGS thin film solar cell structure. This structure consists of a 3µm wide CIGS absorber layer, together with a 50 nm CdS buffer layer and a ZnO window layer. In the p-type absorber layer, a band gap of 1.1 eV and a shallow doping density of 2.1016 cm^{-3} are assumed. In this layer, we present a defect of the type charges: double acceptor (possible charge states (1-, 0), with energy distribution: gauss :Et = 0.60 eV and characteristic energy 0.10 eV above the valence band level and with a defect density of $1.77.10^{13}$ cm^{-3}, the capture constants are shown in Table 1.

Table 1: *Overview of the capture constants used for the SCAPS model.*

Defect (level)	Level (0/−)
c_n (cm^3/s)	5.10^{-12}
c_p (cm^3/s)	10^{-15}

The results are compared with the results of simulation of the same structure but where the single defect acceptor in the layer of shock absorber was replaced with a double defect acceptor and triple defect acceptor, taking account of the degeneration as shown in the equations. All simulations are carried out to 300 K. Results of simulation the capacitance as a function of the frequency (C-f) characteristic under AM1_5G 1 sun.spe illumination conditions are shown in the figure 3.

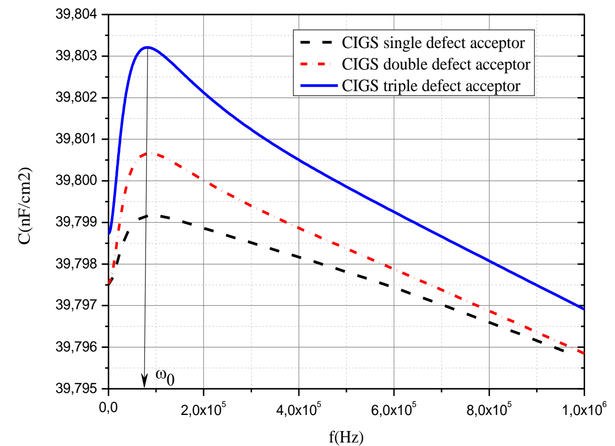

Fig.3*. SCAPS simulation of the capacitance as a function of the frequency (C-f) characteristic under AM1_5G 1 sun.spe illumination conditions. Comparison various models: CIGS single defect acceptor, CIGS double defect acceptor and CIGS triple defect acceptor.*

It is rather common in thin film polycrystalline cells that the capacitance slowly decays over many frequency decades. Changes of capacitance with frequency are normally connected with deep defect states. A single deep defect in the SCR will show up in the *C- f* plot as a sudden transition of one capacitance value to another. The frequency at which the transition occurs is defect number dependent. As can be seen in Fig.1, the *C- f* characteristic of the cells under investigation consists of regionswith varying rate of decreasing capacitance. This could be explained by assuming a band of deep defect states, each with different capture and emission rates, determined by the depth of the state (energetic distance from the band edge). The extent of the decay of the *C- f* curves (at least 4 decades) corresponds to a rather broad band of states. The defect density profiles of the first three situations are shown in Figure 4. Whereas the *C (f)* curves of the CIGS device Figure 3 are dominated by a continuous dispersion that is reflected in a broader defect distribution Figure 4. The decrease of the defect density towards the band edge might also be due to the position of the Fermi level in the bulk of the *p*-type absorber layer, limiting the range in which defects in the lower part of the band gap may be detected.

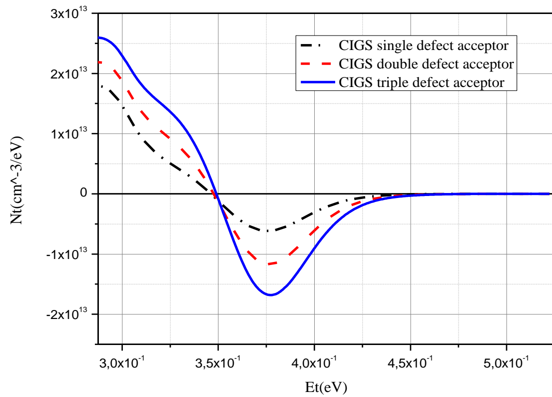

Fig.4 *SCAPS simulation of the defect density per energy as a function of the defect level energy characteristic under AM1_5G 1 sun.spe illumination conditions. Comparison various models: CIGS single defect acceptor, CIGS double defect acceptor and CIGS triple defect acceptor.*

In order to calculate the total contribution of an energy distribution of defects *Nt*(*Et*) this relation still has to be integrated along energy and position. The frequency dependence shows that a defect can contribute to the capacitance if the angular frequency is low enough $\omega \prec\prec \omega_0$ so that the charging and discharging of the defect can follow the applied ac signal. If the angular frequency is too high $\omega \succ\succ \omega_0$, the defect will no longer contribute to th capacitance.Hence, the angular frequency will be assumed t be low enough so that the defect contributes to th capacitance. The impedance spectra are plotted (Figure 5) the complex plane (i. e. Z.re versus Z.im, also known a Nyquist). The extracted device parameters from theoretic fitting of experimental data are listed in Table 2

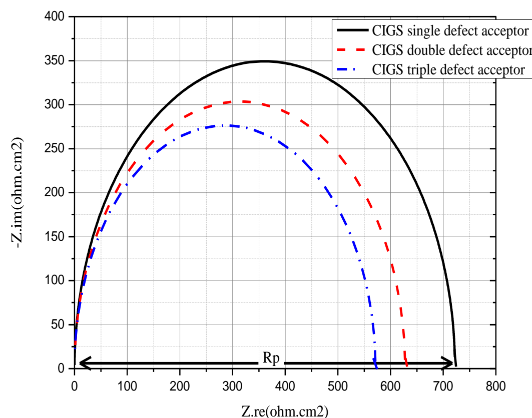

Fig.5 *SCAPS simulation of the impedance spectrum (Nyquist plots) of the polycrystalline CIGS solar characteristic under AM1_5G 1 sun.spe illumination conditions. Comparison various models: CIGS single defect acceptor, CIGS double defect acceptor and CIGS triple defect acceptor.*

TABLE 2: *Values of the parallel resistance and series resistance*

CIGS	Rp (ohm/cm^2)	Rs (ohm/cm^2)
Single defect acceptor	723,89	10^{-18}
Double defect acceptor	629,75	10^{-18}
Triple defect acceptor	571,38	10^{-18}

The Nyquist spectra obtained as a function of the defects number lead to the following observations that is: (1) At low forward the defect number, the resistance and capacitance of n-p junction are dominated by the shunt resistance (RSH) and depletion layer capacitance, respectively, (2) the defects number increases, the radii of Nyquist spectra decreases, indicating the reduction in junction resistance. It must be noted here that the first two observations follow from the description of single time constant (Nyquist spectra below knee voltage of solar cell), and (3), as the junction bias increases beyond the knee voltage, the response of n-p diode junction shifts from high impedance to low impedance due to the switching of the charge accumulation mechanism in the Space charge region (SCR) to the diffusion mechanism in the Quasi neutral region (QNR). The Bode diagram of the phase of the impedance of the solar cell is shown in Fig.6. The Bode diagram of the dynamic impedance phase gives the evolution of the phase as a function of the logarithm of the exciting frequency. The Bode diagram is used to enter the frequency behavior of a system.

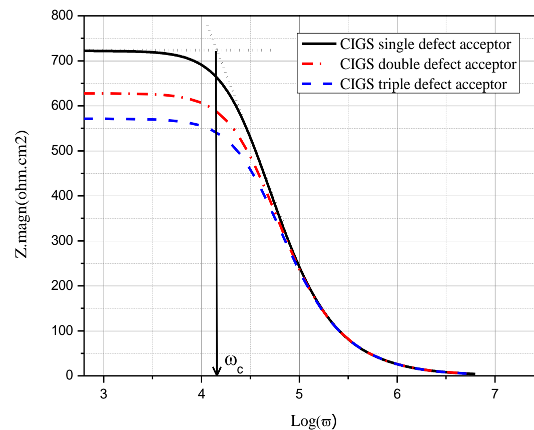

Fig.6 *SCAPS simulation of Modulus of the impedance as a function of the logarithm of the pulsation (ω) characteristic under AM1_5G 1 sun.spe illumination conditions. Comparison various models: CIGS single defect acceptor, CIGS double defect acceptor and CIGS triple defect acceptor.*

TABLE 3: *Values of the cut-off pulsation*

CIGS	Cut-off Pulsation ω_c (rad/s)
Single defect acceptor	1.3995×10^{4}
Double defect acceptor	1.7378×10^{4}
Triple defect acceptor	1.9588×10^{4}

The values of angular frequencies are listed in table 3. For the angular frequencies in the range $0<\omega<\omega_c$, the module of the dynamic impedance of the solar cell is independent of frequency. And the values of the pulse as $\omega> \omega_c$ the impedance modulus decreases with pulsation. Thus the intersection of the extensions of each of the two linear portions of the curve (Figure 6) provides the angular pulse ω_c cut [7]. The lowest the cut-off frequency was obtained to the single defect. This point is determined by the fact that a defect can only contribute to the capacity if the angular frequency is sufficiently low.

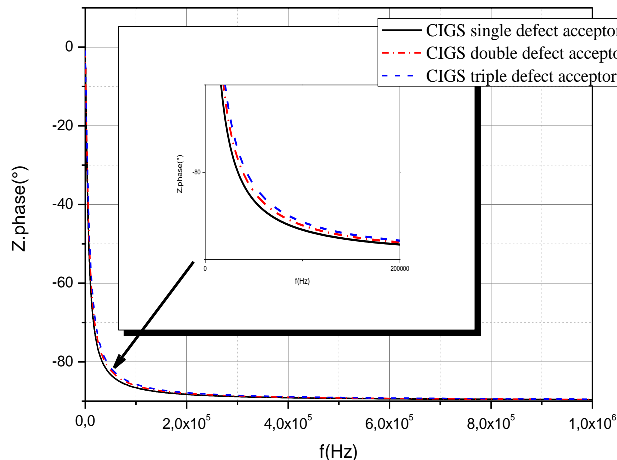

Fig.7 *SCAPS simulation of the phase of the impedance according to the frequency under AM1_5G 1 sun.spe illumination conditions. Comparison various models: CIGS single defect acceptor, CIGS double defect acceptor and CIGS triple defect acceptor.*

The shape of the curves in the figure 7 shows that the phase of the impedance is negative and this confirms the presence of a capacitor in the equivalent electrical model of the solar cell. Thus from the above remarks we propose the following equivalent circuit model:

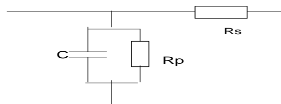

4 Conclusion

The examples given above illustrate the numerical simulation program SCAPS is a valuable tool in modelling defect thin film solar cells based on CIGS. Certain measurements like C-f, parallel resistance and cut-off frequency, have been performed on three different defect in CIGS-thin film solar cells. We noticed that the cut-off frequency increases with the number of defects on the other hand parallel resistance decreases with the number of defect. However, the defect distribution depends significantly on the stoichiometry. A more detailed investigation of the nature of deep-level defects and their role on the recombination process and performance in the CIGS films could further elucidate the material behavior and contribute to improving the performance of CIGS-based cells.

References

[1] C.-T. Sah, W. Shockley, Phys. Rev. 109 (4) (1958) 1103.

[2] R.E.I. Schropp, M. Zeman, "Amorphous and Microcrystalline Silicon Solar cells", Kluwer academic publishers, Norwell, 1998.

[3] S. Siebentritt, U. Rau, "Wide-Gap Chalcopyrites", Springer-Verlag, Berlin Heidelberg, 2006.

[4] M. Burgelman, J. Verschraegen, B. Minnaert, J. Marlein, in M. Burgelman, M. Topič (Eds.), "Proceedings of NUMOS", Gent, B., 2007, p.357

[5] K. Decock, S. Khelifi, M. Burgelman, "Uniform reference structures to assess the benefit of grading in thin film solar cell structures", Proceedings of the 25th European Photovoltaic Solar Energy Conference, Valencia, 2010, pp. 3323-3326.

[6] K. Decock, J. Lauwaert, M. Burgelman, "Modelling thin film solar cells with graded band gap", Proceedings of the 45th International conference on Microelectronics devices and technologies, Postojna, 2009, pp. 245-249.

[7] M. Ndiaye , Z. Nouhou bako, I. Zerbo, A. Dieng, F. I. Barro, G. Sissoko,"determination of electrical parameters of a solar cell under illumination with monochromatic frequency modulation, from diagrams of Bode and Nyquist", J. Sci.Vol. 8, **N° 3** (2008) 59 – 68